ABSTRACT

Title of Document:	Mitigation of Acceleration of Vehicles Subjected to Buried Mine Loading
	Zachary Tyler Plitt, M.S., 2015
Directed By:	Professor William Fourney, Department of Mechanical Engineering

This dissertation investigates the mitigation of acceleration to passengers on a blast loaded vehicle. Small scale explosive testing was conducted to simulate the detonation of a buried mine on a vehicle. Tests were conducted in saturated sand, which will act as the loading mechanism on the simulated vehicle. Piezoelectric accelerometers, in conjunction with high speed cameras, were used to record test data. Two forms of mitigation were utilized in this research: hull shaping and crushing polyurea-coated thin-walled cylinders. Hull shaping deflects the blast, while the polyurea-coated thin-walled cylinders are crushed to absorb energy. Both forms of mitigation were tested, both separately and together, to determine their effectiveness at mitigating acceleration on the simulated vehicle. The goal of this dissertation is to determine the effectiveness of different mitigation techniques at reducing acceleration in order to design safer military vehicles.

MITIGATION OF ACCELERATION OF VEHICLES SUBJECTED TO BURIED MINE LOADING

By

Zachary Tyler Plitt

Thesis submitted to the Faculty of the Graduate School of the
University of Maryland, College Park, in partial fulfillment
of the requirements for the degree of
Masters of Science
2015

Advisory Committee:
Professor William Fourney, Chair
Professor Amr Baz
Professor James Duncan

© Copyright by
Zachary Tyler Plitt
2015

Dedication

This work is dedicated to my parents: to my father, Fred Plitt, for teaching me about work ethic and being an honest man, and to my mother, Kathy Plitt, for teaching me the value of a good attitude and making countless amounts of muffins and chocolate chip cookies over the last year.

This work is also dedicated to my uncle, Bob Kavetsky, for leading me into engineering and, through yardwork, teaching me the Sound Mind Sound Body principle.

Finally, this work is dedicated to my grandfather, John “Sarge” Kavetsky, who I did not have the fortune of knowing but is responsible for instilling all of the values I have learned into my parents and family.

Acknowledgements

First and foremost, I would like to thank my advisor Dr. William Fourney for making all of my research possible. Dr. Fourney gave me endless opportunities in the Dynamic Effects Lab, something that I will always be grateful for. Dr. Fourney was always there with his vast experience and knowledge to show the way whenever the research started seeming impossible. I cannot thank Dr. Fourney enough for all he has done for me in my time at the University of Maryland.

Secondly, I would like to thank my committee members, Dr. Amr Baz and Dr. James Duncan, for their support and insight while completing my dissertation. It would not have been possible without their help.

I would be remiss to not acknowledge Dr. Uli Leiste and Leslie Taylor, two cornerstones in the Dynamic Effects Lab who have seen it all and were always there to lend a helping hand. Your experience and know how in the lab taught me so much.

I would also like to thank all of the undergraduates who assisted me during my time in the Dynamic Effects Lab. A special thanks goes out to two undergraduates, Zach Friedman and Jon Kordell, who were instrumental in completing this thesis and never shied away from the daily rigors that come with small scale explosive testing.

A special thanks goes out to all of the guys who were there with me my first summer in the Dynamic Effects Lab – Tyler Duff, Max Kinsey, and Zach Felder. My first summer working in the lab was so much fun and they were no small part of that. The guys pushed me to keep learning and be better in the lab every day.

And last but certainly not least, I would like to thank Dr. Jarrod Bonsman. Jarrod, affectionately known as J-Rod, has been working in the Dynamic Effects Lab since I showed up and quickly took me under his wing. He allowed me to work side by side with him every day while he worked on his dissertation. He watched me mess up tests and equipment he worked very hard to create, all so I could learn and become a better researcher. It is not much of an exaggeration to say that Jarrod taught me everything I know in the lab. On top of time in the lab, I was Jarrod's teaching assistant for a year, where I learned how to bring enthusiasm into the classroom and how to have fun teaching. Jarrod is someone that I consider to be a great friend, and my time at the University of Maryland would not be possible if not for Jarrod.

Table of Contents

Dedication……ii
Acknowledgements……iii
Table of Contents……v
List of Tables……vi
List of Figures……vii
Chapter 1 – Introduction……1
1.1 Introduction……1
1.2 Background……3
1.3 Small-Scale Testing……5
Chapter 2 – Experimental Set-Up……8
2.1Test Equipment……8
2.1.1 Data Acquisition Equipment……8
2.1.2 Blast Testing Equpiment……13
2.1.3 Moment of Inertia Testing Equipment……17
2.2 Test Set-Up……21
2.2.1 Preparing the Saturated Sand Bed……22
2.2.2 Burying the Explosive Charge……23
2.2.3 Setting the Stand-Off Distance and Saturating the Test Bed……25
Chapter 3 – Experimental Results……27
Chapter 3.1 Flat Bottom Hull versus V-Bottom Hull……27
Chapter 3.1.1 Test Apparatus and Specifics……27
Chapter 3.1.2 Effect of Flat Bottom Hull versus V-Bottom Hu……32
Chapter 3.1.3 Test Repeatability……36
Chapter 3.2 Effect of Off-Center Charges for Flat and V-Bottom Hull……37
Chapter 3.2.1 Test Apparatus and Specifics……37
Chapter 3.2.2 Effect of Off-Center Charges……41
Chapter 4 – Conclusion and Future Work……48
Chapter 4.1 Conclusion……48
Chapter 4.2 Suggested Future Work……48
Bibliography……50

List of Tables

Table 3.1: Test matrix for flat bottom hull versus V-bottom hull study…..……30
Table 3.2: Test results for flat bottom hull versus V-bottom hull……..34
Table 3.3: Test data repeatability for V-bottom, rigid connect……36
Table 3.4: Test matrix for off-center charges study……..……...37
Table 3.5: Tabular results of off-center testing for C.O.G. peak acceleration……...41
Table 3.6: Tabular results of off-center testing for “high side” peak acceleration.….45

List of Figures

Figure 1.1: Effect of MRAPs on IED-caused fatalities [3]……2
Figure 1.2: Comparison of large scale to small scale testing [6]……...7
Figure 2.1: PCB model 350B04 accelerometer. Scale is in inches……9
Figure 2.2: PCB Piezoelectronics Signal Conditioner, Model 438A……10
Figure 2.3: LeCroy oscilloscopes, Model 9314AM and Model 9354AM……10
Figure 2.4: Rubber pad removed from plate (left) and two rubber pads inserted into a test plate (right), one containing an accelerometer and one empty……...11
Figure 2.5: Phantom v12.1 on tripod……12
Figure 2.6: External (left) and internal (right) schematic of RP-501 Detonator [27]……...14
Figure 2.7: Completely made 4.4g (left) and 2.2g (right) charge……...14
Figure 2.8: FS-17 Firing Module……15
Figure 2.9: Test bed showing hanging chains, net, and water tube……....17
Figure 2.10: Schematic showing connections between camera, oscilloscopes, firing box, and accelerometers……...…17
Figure 2.11: CAD model of V-bottom hull……18
Figure 2.12: V-shaped bottom showing holes drilled through center of gravity……..19
Figure 2.13: V-shaped bottom with hanging mass and tracking target attached……...20
Figure 2.14: Phantom v12.1 cameras tracking both hanging mass (lower camera) and plate rotation (higher camera)……20
Figure 2.15: Phantom v12.1 tracking rotational velocity of plate……..21
Figure 2.16: Prepared test bed, showing aluminum scraper……...23
Figure 2.17: Charge burial template showing five charge burial locations……..24
Figure 3.1: Dimensioned CAD sketch of V-bottom hull (dimensions in millimeters)……..……...28
Figure 3.2: Polyurea coated can without inserted "can top"……30
Figure 3.3: Flat bottom hull with rigid connectors (left) and V-bottom hull with rigid connectors (right)……..……...31
Figure 3.4: Sample acceleration versus time plot……....33
Figure 3.5: Test results for flat bottom hull versus V-bottom hull……..…34
Figure 3.6: Peak acceleration reduction for centered charge location……..35
Figure 3.7: Placement of charges and accelerometers for ¼ Front and ½ Front…..39
Figure 3.8: Placement of charges and accelerometers for ¼ Right and ½ Right……40
Figure 3.9: Center of gravity peak acceleration data for off center charges……..43
Figure 3.10: Center of gravity peak acceleration reduction from baseline……44
Figure 3.11: Peak acceleration data for the "high side"……46
Figure 3.12: Peak acceleration reduction from baseline for the "high side"…….46

Chapter 1: Introduction

1.1 Introduction

A surge in mine related deaths in Middle Eastern conflicts over the past few years has prompted research into the mitigation of the impact on a blast loaded vehicle. In past military conflicts, it has been observed that blast loading can cause brain damage, but the exact cause was unknown [1]. The recent rise in deaths due to Improvised Explosive Devices (IEDs) has led to research that has speculated that the high acceleration experienced by soldiers on a blast loaded vehicle leads to Traumatic Brain Injury (TBI) [2]. This research aims to design vehicles that can reduce the peak acceleration for passengers on board the vehicle, in the event that the vehicle is blast loaded by an IED. As a country, the United States has a moral imperative to defend its soldiers as well as it can against known threats such as the IED.

The answer to the high number of IED related casualties has been vehicle design. Mine-Resistant Ambush Protected Vehicles, or MRAPs, have been implemented in war zones and resulted in a great reduction of casualties. MRAPS use an angled bottom, not unlike the V-bottom hull used in this research, to deflect ejected soil away from the vehicle, reducing upward acceleration. The effectiveness of MRAPs in reducing IED related casualties is displayed in Figure 1.1 [3].

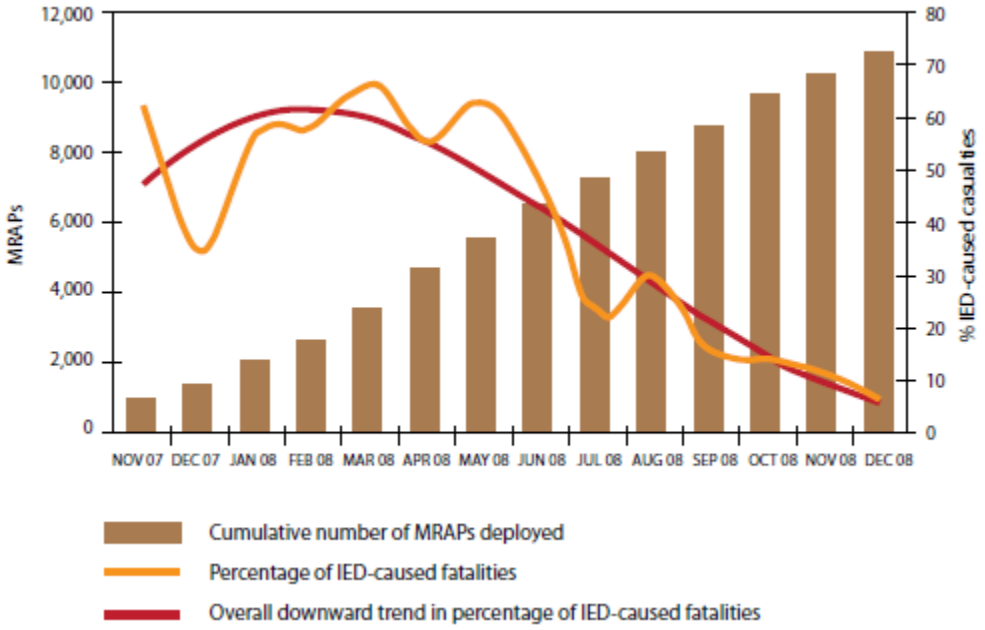

Figure 1.1: Effect of MRAPs on IED-caused fatalities [3]

As can be seen in the seen in Figure 1.1, as the number of MRAPs deployed in the field has increased, the percentage of IED-caused fatalities has sharply decreased. While these soldiers are surviving the blast event, they are not wholly protected from brain damage by MRAPs and can return home with TBI. Safer military vehicles that protect soldiers from blast-related TBI can improve the quality of life for said soldiers, allowing them a smoother and more productive transition into civilian society. Not only is there a great moral incentive to researching safer military vehicles, but there is a great financial incentive as well. The VA projects the 10 year costs of TBI from 2016 to 2025 to be 2.2 billion dollars [4]. While IED blasts are certainly not the only cause of TBI, they are a contributing factor. Reducing the number of TBI related to IED blasts could certainly reduce military related health care costs well into the future.

Designing safer military vehicles is not a simple task. One tried and true method of reducing acceleration on a military vehicle is to raise the chassis height of the vehicle. This added distance between the explosive charge and the vehicle provides a layer of safety, but not without cost. Added chassis height increases the chance of vehicle rollover, a large concern in a war zone. MRAPs can weigh upwards of 30 tons, making rollover especially dangerous. Of 38 MRAP incidents between November 2007 and June 2008, only four did not involve rollover [5]. While MRAPs are certainly a good defense against IEDs, the design can still be improved.

At the Dynamic Effects Lab at the University of Maryland, small-scale explosive testing is done to simulate the blast loading of military vehicles. A simulated vehicle was designed to measure the peak acceleration experienced by a full scale military vehicle. Two different mitigation techniques were used in these simulated tests. The first mitigation technique is hull shape. Both a flat hull and a V-bottom hull were tested to measure their effectiveness at reducing the peak acceleration of the simulated vehicle. The second mitigation technique was polyurea-coated thin-walled cylinders. These polyurea-coated thin-walled cylinders are crushed by the blast, which absorbs energy and reduces acceleration. These two mitigation techniques were tested, both individually and together, to measure their effectiveness. These mitigation techniques were tested by charges placed both under the center of the vehicle, as well as four off-center charge locations. These tests provided a wide array of data on how these mitigation techniques perform under multiple circumstances.

1.2 Background

At the Dynamic Effects Lab, a great deal of work has been done with respect to both understanding the physical conditions of blast loading, as well as how to mitigate the acceleration of blast loading. The mechanisms of plate loading that occur during an explosive test have been studied [6]. Different mitigation techniques, such as angled and composite hulls, have also been investigated [7, 8]. The main takeaway from this research is that the simulated vehicle is loaded by sand or other soil ejected at a high velocity by the charge. This soil has been shown to be traveling at a velocity greater than Mach 1. When this soil hits the simulated vehicle or test plate, large pressures develop and cause the motion of the plate [9].

In order to further reduce the acceleration of a blast loaded vehicle, other mitigation methods have been created. The other method utilized in this research is the crushing or buckling of tubes and cylinders to absorb energy from the blast. The crushing and collapsing of tubes, of all different kinds of geometries, materials, loading conditions, and boundary conditions, has been thoroughly investigated. [10, 11, 12]. This includes cases relevant to this research, like dynamically loaded impact and composite structures [13, 14]. The crushing of metal beverage cans, very similar to the crushing of thin-walled cylinders done in this research, has been tested [15]. The use of these structures has been both numerically and experimentally investigated as use for sacrificial claddings for structures undergoing blast loading [16, 17]. All of this is to say that using a thin-walled cylinder to mitigate a dynamic load is not something new or unexplored. The buckling of these thin-walled structures clearly exhibits a benefit when attempting to mitigate dynamic loading.

The other area of interest when it comes to this research is the behavior of polyurea. Polyurea coatings are often used in blast applications as a form of mitigation. The deformation of polyurea, as well as how polyurea performs under a high strain rate [18], has been investigated. Most importantly for this research, how polyurea behaves as a blast resistant material [19] has also been researched. Polyurea behaves as a rubbery material at low strain rates, but exhibits a "glassy" behavior when subjected to high strain rates [20], typical of a blast loaded vehicle. Polyurea, while explored widely elsewhere, has also been explored at the Dynamic Effects Lab. In previous work, the hull of a simulated vehicle was coated in polyurea, which was an effective way to mitigate acceleration [21].

Other previous work done by Dr. Jarrod Bonsmann at the Dynamic Effects Lab has deeply investigated the effect of crushing thin-walled cylinders, both with and without a polyurea coating. Research into the number of cans, can geometry, and polyurea coating was conducted with the goal of maximizing the mitigation of acceleration on a blast loaded vehicle. [22]. Dr. Bonsmann concluded that polyurea-coated thin-walled cylinders could be used to drastically reduce the peak acceleration of a blast loaded military vehicle.

1.3 Small Scale Testing

The Dynamic Effects Lab at the University of Maryland conducts small scale explosive testing. Testing at small scale has multiple advantages. Explosive tests can be run in less time and for a lower cost than large scale testing, providing a greater amount of data. Small scale testing has been shown to accurately depict the response

of a target plate to an explosion at large scale [23, 24]. Explosive tests are done at small scale, and then compared to large scale testing using a scaling factor (SF). The equation for calculating the scaling factor is shown below.

$$SF = \left(\frac{mass_{full\ scale}}{mass_{small\ scale}}\right)^{\frac{1}{3}}$$

Using the scaling factor, length and time can be scaled between small scale and full scale testing. For example, in this research, a small scale charge of 4.4 grams is scaled to a full scale charge of 4.5436 kilograms (10 pounds). This results in a scaling factor of 10. Full scale length and time is determined by multiplying the small scale length and time by the scaling factor. This means that, for this research, peak acceleration values at small scale are divided by 10 to calculate the full-scale acceleration value.

To prove that small scale explosive testing is accurate, work done at the Army Research Laboratory (ARL) in Aberdeen, MD, was compared to small scale testing done in the Dynamic Effects Lab. Full scale testing utilized two different charge sizes: 2.27 kilograms and 4.54 kilograms of TNT. The depth of burial of the charge, as well as the stand-off distance of the test plate, was also altered to provide multiple different testing conditions. Test results can be seen in Figure 1.2 [6], which compares testing done at small scale in the Dynamic Effects Lab to full scale testing done at ARL. . The test information is shown for each test. Tests 1 and 6, as well as tests 4 and 4a, are repeats or each other.

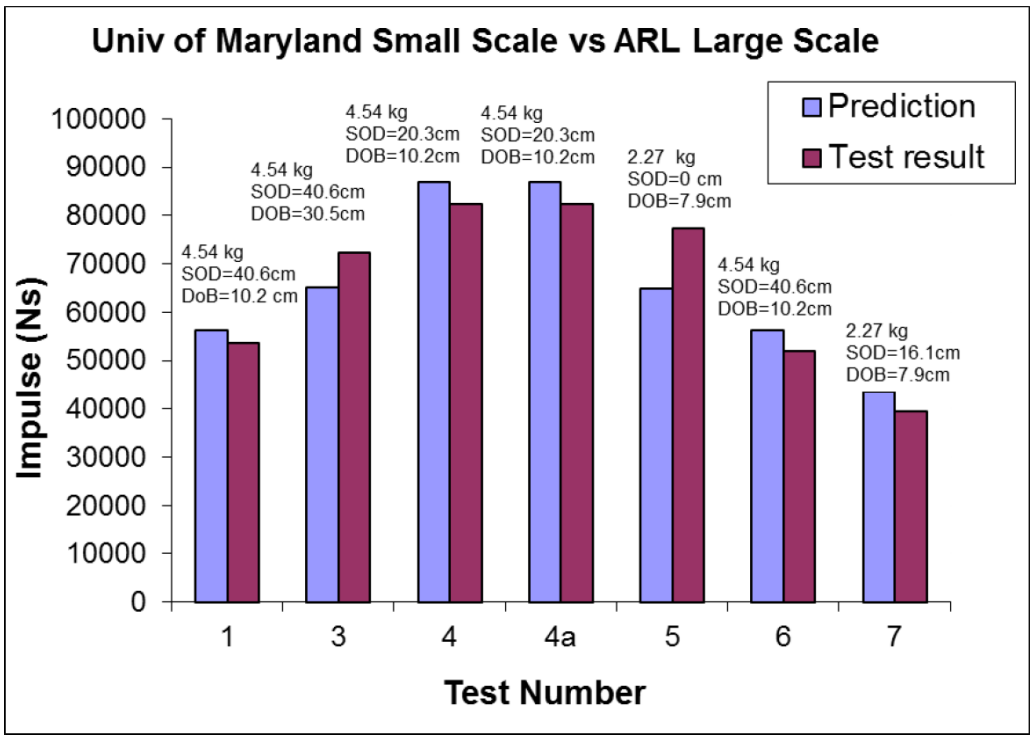

Figure 1.2: Comparison of large scale to small scale testing [6]

Chapter 2 – Experimental Set-up

2.1 Test Equipment

There are two categories of equipment needed to perform these explosive experiments: data acquisition equipment and blast testing equipment. In addition, for this particular series of testing, another set of equipment had to be constructed to experimentally confirm the rotational moment of inertia of our test plates. The equipment used is outlined below.

2.1.1 Data Acquisition Equipment

Two types of data were acquired during blast testing: accelerometer data and camera data. Camera data is used to confirm accelerometer data, as both independent sets of data should match when compared if they are accurate. Only one type of accelerometer was used during testing. The accelerometer was manufactured by PCB Piezotronics Inc, model 350B04. This accelerometer has a measurement ranged of ±5000 g's and can produce 10,000 samples per second [25]. An accelerometer is shown in Figure 2.1.

Figure 2.1: PCB model 350B04 accelerometer. Scale is in inches

To ensure that the accelerometer signal is properly acquired, a PCB Piezoelectronics Inc. signal conditioner, model 483A, is used. The signal conditioner assists in preparing the signal for recording, as well as providing the correct excitation power for the accelerometers. The signal conditioner is shown in Figure 2.2. The accelerometers are directly connected through cables to the signal conditioner to a specific channel. These signals are then split and sent to oscilloscopes for recording. Two oscilloscopes manufactured by LeCroy, model numbers 9314AM and 9354AM, are used. The oscilloscopes record from one mega-sample per second to five mega-samples per second, which is two orders of magnitude greater than our accelerometers can produce. Both oscilloscopes are shown in Figure 2.3. For every blast test, voltage ranges were set on the oscilloscopes corresponding to the expected acceleration value recorded by the accelerometers. Each oscilloscope had four possible channels, providing eight total channels to record data. The data from the two accelerometers was split between the eight channels, providing four voltage settings for each accelerometer. This allowed for safety channels, which could be set to high voltage settings to ensure that our data was recorded in the case of a bad

prediction or equipment malfunction. While there are eight total channels on the oscilloscope, only two were downloaded and analyzed for every test.

Figure 2.2: PCB Piezoelectronics Signal Conditioner, Model 438A

Figure 2.3: LeCroy oscilloscopes, Model 9314AM and Model 9354AM

To ensure an accurate signal, the accelerometers were inserted into the test plate using rubber pads. One inch polyurethane sheets of durometer hardness 60A were purchased from McMaster-Carr, which were then machined to proper size to fit

in a 9/16 inch hole in the plate. The rubber pad was inserted into the plate, and then the accelerometer was pushed into the rubber pad. The rubber pad holds the accelerometer very tight, ensuring that the accelerometer does not move inside the pad and that the accelerometer signal is an accurate representation of the motion of the test plate. The rubber pad acts as a mechanical filter, removing some plate vibration from the accelerometer signal. Using these rubber pads is an established practice in the Dynamic Effects Lab, and has been shown not to alter test results [26]. Figure 2.4 shows a rubber accelerometer pad, as well as how the accelerometer pads are inserted into a test plate.

Figure 2.4: Rubber pad removed from plate (left) and two rubber pads inserted into a test plate (right), one containing an accelerometer and one empty

To obtain camera data, a Phantom v12.1 high speed camera was equipped with a Tamron 28-75mm variable focus lens. The camera is placed on a tripod so that the camera can properly view the test. At reduced resolution, the v12.1 has the capacity to capture one million frames per second. The v12.1 also has the capacity to film at a maximum resolution of 1280 x 800 pixels. Figure 2.5 shows the Phantom v12.1 on a tripod, as it would be situated for testing.

Figure 2.5: Phantom v12.1 on tripod

For blast testing, the resolution and recording speed are adjusted depending on the test, maxing out the frame rate for the chosen resolution. The frame rate for these blasts tests was typically around 18,000 frames per second. The Phantom v12.1 is attached to a laptop computer through an Ethernet cable. Phantom software is installed on the laptop computer to allow for the adjustment of camera settings, as well as downloading the test video onto an external hard drive for later analysis.

After the data from both the accelerometers and the camera is saved onto an external hard drive, it is processed using two separate programs. To analyze the camera data, Phantom Control Software is utilized. Phantom Control Software allows the user to record displacement versus time data of a given point for each frame taken. The displacement versus time points are saved onto a file, which can then be opened in Microsoft Excel. These displacement versus time files can then be further analyzed in Excel to provide more useful data.

Accelerometer data is processed in UERD Tools, a program developed by NSWC – Carderock Division. UERD Tools allows the user to manipulate the accelerometer signals with mathematical functions such as integration and filtering. The accelerometer signals are twice integrated to produce a displacement versus time profile for the test. The displacement versus time profile from the accelerometer data is compared in UERD Tools to the displacement versus time profile of the camera data. If the accelerometer data is accurate, it should match the camera data. This confirms that the accelerometer reading is accurate.

2.1.2 Blast Testing Equipment

The explosive charges used in blast testing were created using the exact same process every time to ensure test repeatability. The explosive used was Deta Sheet, manufactured by Omni Explosives. Deta Sheet is a plastic explosive sheet that contains 63% of its mass in PETN, a high explosive, and 37% of its mass in plasticizer. For each charge, a prescribed amount of Deta Sheet is pressed into a delrin casing, which allows for constant charge geometry between tests.

After the Deta Sheet has been pressed into the casing, a detonator is inserted one-third of its length into the charge. The detonators used were Exploding Bridge Wire (EBW) Detonators manufactured by Teledyne RISI, model RP-501. The detonators contain 227 milligrams of RDX and 136 milligrams of PETN. The 136 milligrams of PETN, along with the 227 milligrams of RDX, combines with the PETN in the Deta Sheet, summing to a total explosive weight used to define the charge. The detonator is then held into place by an epoxy. After the epoxy has dried,

thin wooden sticks are attached to the charge to ensure that the charge remains at a fixed depth and in the correct orientation during charge burial. Figure 2.6 shows both the internal and external schematic of a RP-501 EBW detonator, while Figure 2.7 shows complete 4.4 gram and 2.2 gram charges.

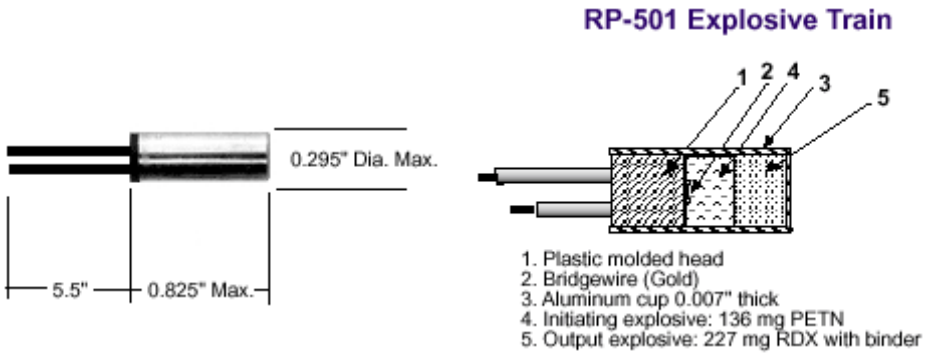

Figure 2.6: External (left) and internal (right) schematic of RP-501 Detonator [27]

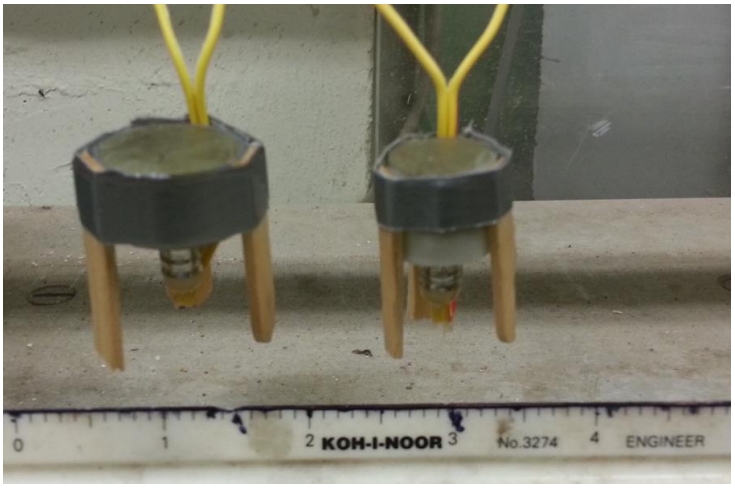

Figure 2.7: Completely made 4.4g (left) and 2.2g (right) charge

To detonate the charge, an FS-17 firing system manufactured by Reynolds Industries Incorporated is utilized. The firing module is capable of producing a 4000 volt pulse. The firing system is connected to the detonator, high speed camera, and

oscilloscopes. When the 4000 volt pulse is delivered by the firing system, the camera and oscilloscopes are triggered to begin recording data and the charge is detonated. The firing system ensures that data recording and charge detonation begin simultaneously. An FS-17 firing module is shown in Figure 2.8.

Figure 2.8: FS-17 Firing Module

Testing takes place in a square steel tank with sides of length of 1.5 meters. A system has been designed to allow the saturation of sand in this tank. A pipe is attached to the bottom of the tank, allowing water to flow in and out to saturate the sand. The bottom of the tank is filled with rocks covered by a thin mesh, which allows the tank to fill with water without allowing sand to clog the pipe. On top of the mesh netting is the sand, which becomes saturated at the time of the test. A cylinder connected to the water pipe, which allows water to flow into the tank from a hose and allows for minor adjustments in water height. This cylinder ensures that the height of the water is consistent from test to test.

To hold the plate in place during testing, four chains hung from the ceiling are utilized. These chains are fitted with a double turn-buckle eye-hook, as well as an S-hook. The double turn-buckle eye-hook allows for the adjustment of the length of the chain, ensuring that the plate is hung the proper distance from the sand. The S-hook is attached at the end of each chain, and can be hooked onto the plate to connect the chain and the testing plate. Above the test bed is a protective net, which protects the test plate from hitting the ceiling in the event that the plate is accelerated very harshly. This is not common for the larger plates utilized in this battery of testing. Figure 2.9 shows the test bed set-up, including the chains and the water tube. Figure 2.10 is a schematic of the total test set-up, incorporating the camera and the oscilloscopes.

Figure 2.9: Test bed showing hanging chains, net, and water tube

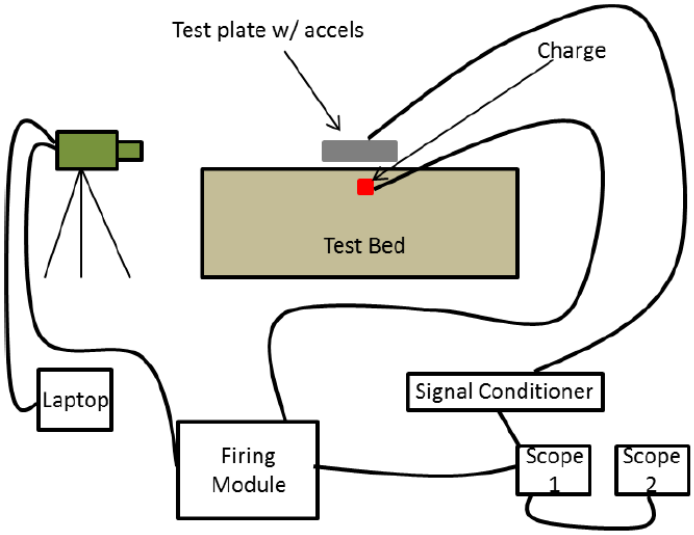

Figure 2.10: Schematic showing connections between camera, oscilloscopes, firing box, and accelerometers

2.1.3 Moment of Inertia Testing Equipment

For the rectangular hull and V-shaped hull, theoretical moments of inertia could be calculated. But to ensure that the actual moments of inertia matched the theoretical values, a test set-up had to be designed to confirm that the values matched. First, to calculate the theoretical moments of inertia of the V-shaped hull, a CAD model of the V-shaped hull was produced. The model is shown in Figure 2.11.This model provided the theoretical moments of inertia for the V-shaped hull. Theoretical moments of inertia for the rectangular hull are easily calculated through established formulas.

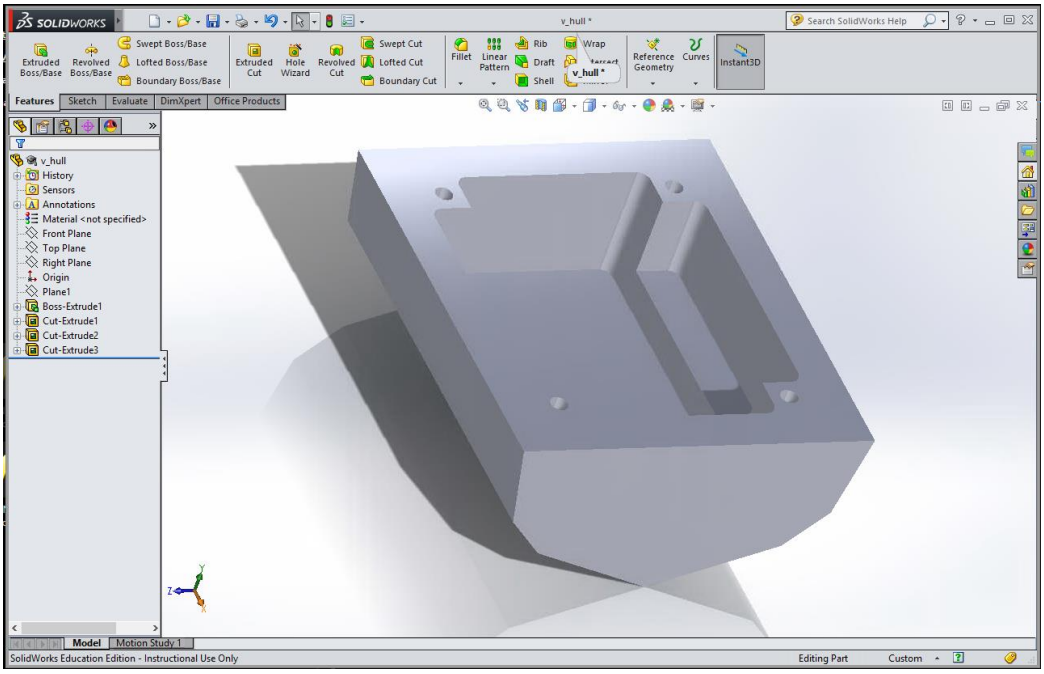

Figure 2.11: CAD model of V-bottom hull

After theoretical values had been determined, the plates were prepared for testing. Holes were drilled through the plates center of gravity and through the established “x” and “y” axis. The plates were then attached to a rod through the given axis, which allowed us to calculate the moment of inertia about that axis. The rod was then attached to a fixed set-up using two ball bearings, which caused the axis to be

fixed in space but allowed the plate to rotate about the fixed axis with negligible friction. A hole drilled through the y-axis, as well as how the plate is supported through the x-axis, is shown in Figure 2.12.

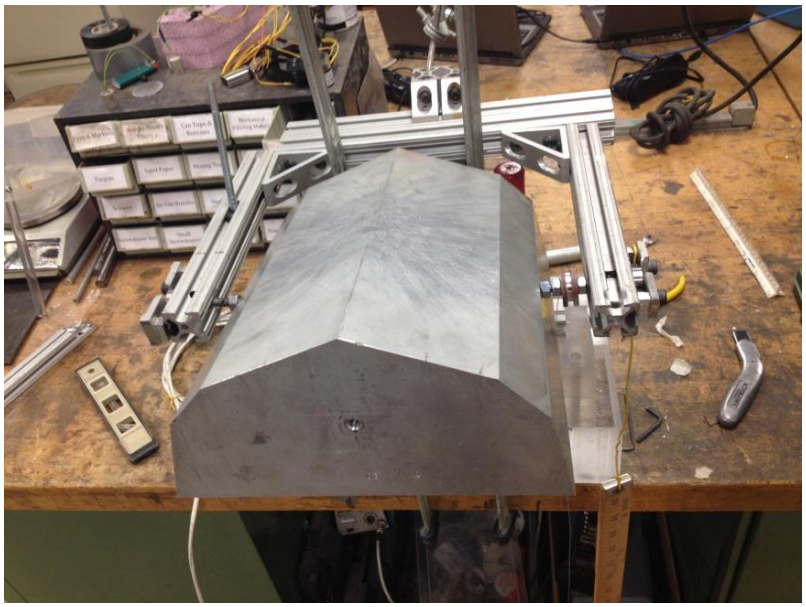

Figure 2.12: V-shaped bottom showing holes drilled through center of gravity

To determine the moment of inertia, a torque was applied to the plate using a hanging mass. The mass hung at a fixed distance from the rotational axis. Figure 2.13 shows the hanging mass. The mass would then accelerate due to gravity, applying a varying force. A Phantom v12.1 camera tracked the displacement of this hanging mass, allowing for the calculation of the acceleration of the hanging mass and therefore the force applied. A torque was calculated by multiplying this force by the set distance.

Figure 2.13: V-shaped bottom with hanging mass and tracking target attached

Figure 2.14: Phantom v12.1 cameras tracking both hanging mass (lower camera) and plate rotation (higher camera)

To track the rotational velocity of the plate, another Phantom v12.1 camera filmed the rotation of the plate. A target was attached to the plate, which would pass by the camera every revolution. The time of these revolutions was recorded in the Phantom Camera Control software, which was then exported to Microsoft Excel. The

rotational velocity of the plate, as well as the motion of the hanging mass, was incorporated into a work-energy relation that allowed for the calculation of the moment of inertia of the plate. Four moments of inertia were calculated: the moment of inertia about the x and y axis for the rectangular hull, and the moment of inertia about the x and y axis for the V-shaped hull. These experimental values confirmed the theoretical values, and the experimental values were then used in later data calculations. The camera set-up for the moment of inertia tests can be seen in Figures 2.14 and 2.15.

Figure 2.15: Phantom v12.1 tracking rotational velocity of plate

2.2 Test Set-Up

To ensure test consistency, there are a few steps that are unchanged between tests. A test bed is prepared from scratch in a set manner. A charge is then buried in the test bed and the test bed is saturated. Once the test bed has fully saturated, the

blast test is conducted and the test bed is allowed to drain before the test bed is demolished and reformed before the next test.

2.2.1 Preparing the Saturated Sand Bed

When the test bed is unformed, the 1.5 meter by 1.5 meter steel tank contains sand in no prior shape or compaction. To begin forming the test bed, a 1.2 meter by 1.2 meter elevated platform is formed in the center of the steel tank by removing sand from the sides and moving it into the center. The test bed is then hand molded to form the elevated platform, with the sand leveled by the person making the test bed. After the elevated platform has been made, the platform is compacted using a cinder block. The elevated platform is impacted by the cinder block a set number of times in a consistent pattern, allowing for consistent compaction between tests. After the first layer is compacted, the surface is roughed up to ensure proper meshing with the second layer. To form the second layer, more sand is removed from the outside edges and piled into the middle, where it is again hand formed and leveled to be compacted. The cinder block is again used to compact the second layer, in the same manner of the first layer. After both layers are completed, the test bed is leveled with an aluminum scraper. This scraper allows for a consistent height of the elevated sand platform. Once the sand platform has been leveled, a wood block is used to smooth the surface of the platform and remove minor defects. A prepared test bed can be seen in Figure 2.16.

Figure 2.16: Prepared test bed, showing aluminum scraper

This technique allows for a consistent test bed that improves the repeatability of the blast testing.

2.2.2 Burying the Explosive Charge

Once the test bed has been prepared, the charge is buried. For this particular battery of testing, there were charges placed both under the center of the plate and off-center of the plate, depending on the test conducted. To ensure that the charge is buried in the right place with respect to the test plate, a template was made using a CNC machine. This allowed for consistent charge burial no matter the charge location. The charge burial template is shown in Figure 2.17.

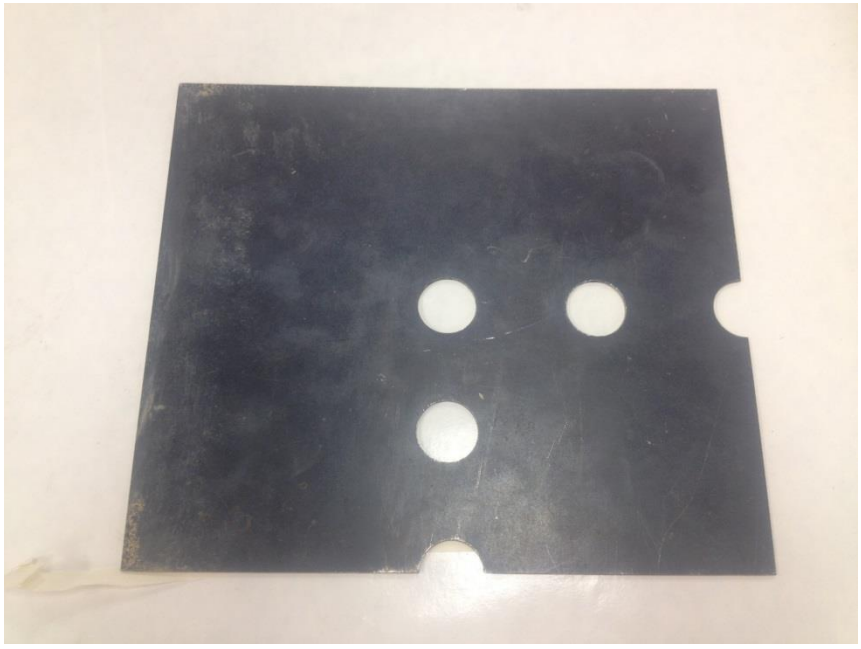

Figure 2.17: Charge burial template showing five charge burial locations

First, the plate was hung in the center of the test bed using the chains hanging from the ceiling. The outline of the plate is then traced into the surface of the sand. The test plate was then removed, and the template placed inside the outline of the test plate. For every test, the template should fit exactly into the test plate outline, as they are exactly the same dimensions. With the template in place, a corer was used to remove the amount of sand necessary to place the charge. The corer was placed through the correct hole in the template and pressed straight down into the test bed. With the sand now removed, the charge is gently placed into the hole, and then tapped to the correct depth of burial (DOB) with a hammer. Depth of burial can be described as the distance between the top of the buried explosive and the top of the sand test bed. The depth of burial is then checked to be exactly 10 millimeters from the surface of the test bed using calipers for every test outlined in this thesis.

After the charge has been inserted to the proper depth of burial, the lead wires connecting the detonator to the trigger box are run along the surface of the sand to the edge of the steel test bed. The lead wires are then folded over the edge and held in place using a piece of duct tape. After the lead wires are taped to the side of the test bed, the top of the charge is covered with loose sand from the outer edge of the test bed. The sand is pressed into the hole and impacted with a wooden block. A set number of hits are delivered to the sand to ensure test consistency. Once the sand has been compacted on top of the charge, the excess sand is smoothed away using the wooden block. When the charge has been buried and the test bed surface has been returned to level, the bed can be saturated.

2.2.3 Setting the Stand-Off Distance and Saturating the Test Bed

The stand-off distance (SOD) of a plate is determining by measuring the distance between the top of the test bed surface and the lowest point on the test plate. For the rectangular hull, the SOD can be measured to any point on the bottom of the test plate. For the V-shaped hull, the SOD is measured to the bottom of the V, the lowest point on the test plate. To set the SOD, the plate is hung from the ceiling chains and adjusted using the double turn-buckle eye-hooks until the plate is level and at the correct height. After the plate is hung to the correct height, it is checked that the plate hangs directly over the outline drawn in the sand while burying the explosive charge. This ensures that the plate hangs in the correct spot so that the charge impacts the plate at the desired location.

After the charge has been buried and the plate has been hung in the correct location, the test bed is saturated. Water enters the cylindrical tube to the side of the bed through a hose, where the water flows into the pipe at the bottom of the steel tank. This allows the tank to saturate fully from the bottom. Water is allowed to enter the tank until the water reaches the proper height in the steel tank. Water height is held consistent between tests. The sand bed is then allowed to saturate for 30 minutes, the amount of time necessary to fully saturate the sand.

After the test bed has saturated, two dummy charges are fired using a spark head. This ensures that the cameras and oscilloscopes begin recording data at the same time the charge has been detonated. If both dummy charges have been successfully fired, the explosive charge is connected to the firing box and detonated. Data is then saved from the camera using Phantom Control Software and from the oscilloscopes. This data is saved to an external hard drive for processing utilizing UERD Tools and Microsoft Excel.

Chapter 3 – Experimental Results

Chapter 3.1 Flat Bottom Hull versus V-Bottom Hull

The first battery of testing was conducted to determine the effect of both hull shaping and polyurea-coated cans on mitigating acceleration. Hull shaping and polyurea-coated cans were tested individually and together to determine their effectiveness at mitigating acceleration.

3.1.1 Test Apparatus and Specifics

Before explaining the results of the flat bottom versus V-bottom tests, the test specifics for these tests first will be discussed. Each test contains three elements: a frame, a hull, and connections between the frame and the hull. These components possess geometries similar to those used for military vehicles, scaled down for small scale testing. The frame represents where the passenger of the vehicle would sit. The same frame is used for every test. The rectangular frame is 251.9 millimeters long by 219.5 millimeters wide, with a height of 38.1 millimeters. There are holes drilled into the frame which allow for the insertion of the accelerometers. There are also four tracking targets screwed into the top of the frame, to allow for accurate tracking of the plate. The tracking targets are attached to the frame using eye-bolts, which are used to hang the plate from the ceiling. The frame is made from solid aluminum and weighs 6.02 kilograms with all of the tracking targets attached.

The second element is the hull. The hull represents the bottom of a military vehicle. Two different hulls are used in this testing: the flat bottom rectangular hull and the V-bottom hull. The flat bottom rectangular hull is identical in geometry to the

rectangular frame, the only difference being a reduced weight of 5.67 kilograms because the hull does not have tracking targets attached. The V-bottom hull has an identical geometry at the top as the rectangular frame and hull, 251.9 millimeters long by 219.5 millimeters wide. Instead of a rectangular shape, the hull has a V shape intended to deflect the explosive blast. The geometry of the V-bottom hull can be most clearly described in Figure 3.1.

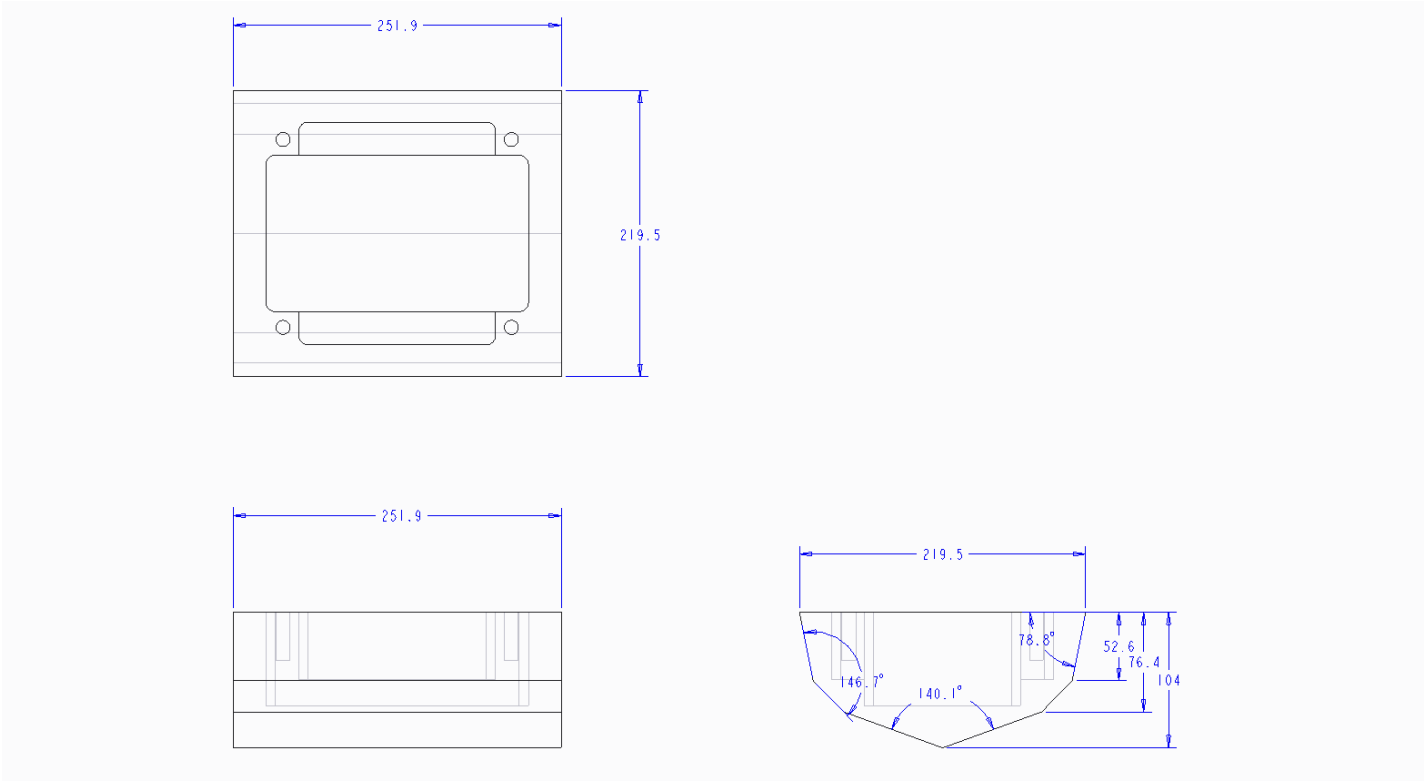

Figure 3.1: Dimensioned CAD sketch of V-bottom hull (dimensions in millimeters)

The V-bottom hull displayed above has a dihedral angle, or the angle between the normal and the bottom edge of the plate, of 20 degrees. A dihedral angle of 20 degrees was shown, in previous work at the Dynamic Effects Lab, to reduce the impulse on a test plate by up to 45% [7].

The final element of the test is the connection between the frame and the hull. Four holes are drilled in the corners of the frame and both hulls, which allows for a consistent and evenly distributed connection between the two plates. There are two different connections used in this testing: rigid steel connection and polyurea coated can connection. The rigid steel connectors are 38.1 millimeters high (1.5 inches) and made of solid steel. These connectors do not deform under this circumstance and behave rigidly. The rigid steel connectors are not meant to provide mitigation but just to establish a solid connection between the frame and the hull.

The second connector used is the polyurea coated can. The polyurea coated can is a cylinder 38.1 millimeters high with a diameter of 50.8 millimeters, and is made using .004 inch thick aluminum shim stock. The shim stock is evenly coated with 5 grams of HM-VK Ultra High Strength Handmix Polyurea Elastomer, made by Specialty Products Inc. (SPI). The HM-VK, in combination with the aluminum shim stock, creates a lightweight structure that possesses large amounts of strength in a high strain rate environment. When these cans are loaded by the blast, they will deform, absorbing energy from the blast and mitigating the acceleration on the frame. The polyurea coated can is connected to the hull and the frame using two "can tops." Precisely sized tops fit into the top and bottom of the can, which are then screwed tightly into the hull and the frame. Note that both the rigid connector and the polyurea coated can connector 1.5 inches tall, providing identical plate geometry at the start of each test. One polyurea coated can is shown in Figure 3.2.

Figure 3.2: Polyurea coated can without inserted "can top"

Table 3.1 is the test matrix for the first series of testing.

Test Number	Charge Location	Hull	Connection
1	Center	Flat Bottom	Rigid
2	Center	V-Bottom	Rigid
3	Center	Flat Bottom	Polyurea Coated Cans
4	Center	V-Bottom	Polyurea Coated Cans

Table 3.1: Test matrix for flat bottom hull versus V-bottom hull study

Figure 3.3 illustrates two of the four test arrangements utilized. The flat bottom hull with the rigid connectors, as well as the V-bottom hull with the rigid connectors, can be seen below. The frame is connected to the hull with four rigid connectors, with one connector in each corner. The rubber accelerometer pads, as well as the four tracking targets, can also be seen.

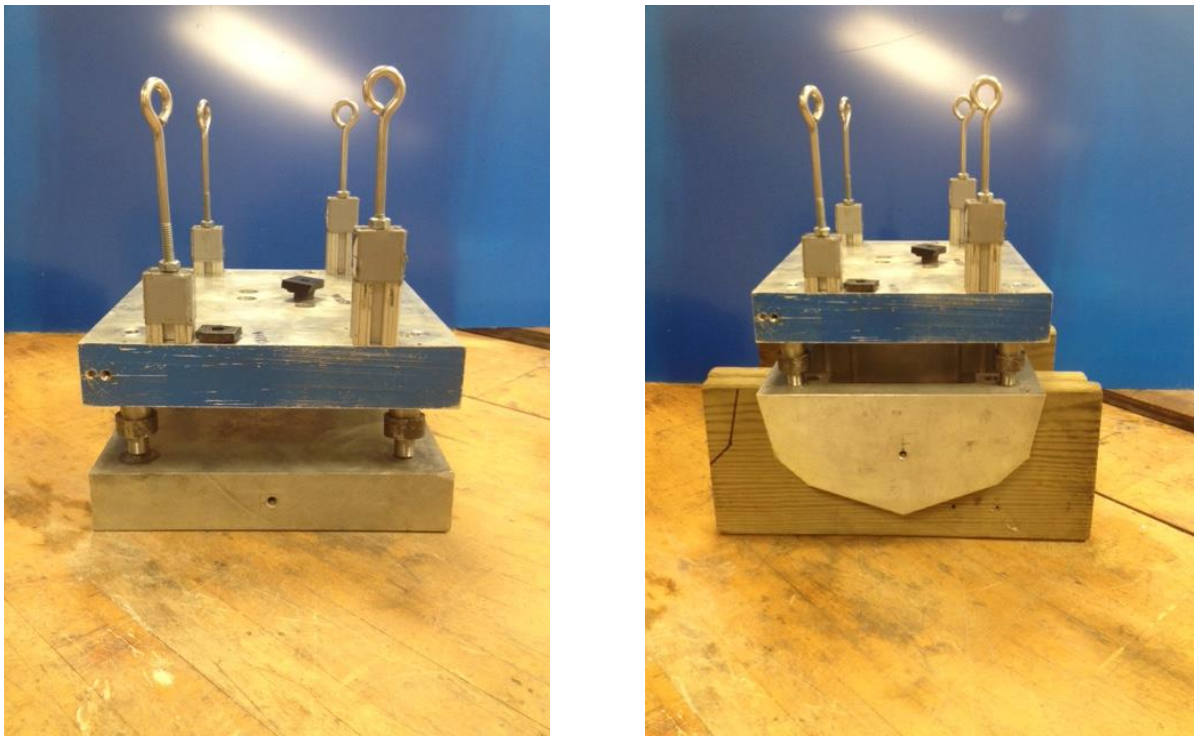

Figure 3.3: Flat bottom hull with rigid connectors (left) and V-bottom hull with rigid connectors (right)

To conduct the test, the plate is hung from the ceiling using chains. The charge is buried in the center hole of the charge template, placing the charge directly in the geometric center of the hull and frame. The accelerometers are placed equidistant from the center line into the rubber pads. No rotation is expected in this series of tests. For every test, a 4.4 gram charge is used. A consistent test arrangement consists of a 10 millimeter depth of burial and a 40 millimeter stand-off distance. For

every test, the plate is loaded identically. The only variables are the changing hull shape and connectors.

3.1.2 Effect of Flat Bottom Hull versus V-Bottom Hull

The main concern when dealing with Traumatic Brain Injury is the peak acceleration felt by soldiers on the vehicle. In order to see the peak acceleration of the frame, the acceleration signals were analyzed in UERD Tools. One sample acceleration versus time plot from this series is displayed in Figure 3.4. The peak acceleration of the two accelerometers was averaged to produce the peak acceleration of the center of gravity. The two accelerometer signals had close peak acceleration values, as there was no plate rotation in these tests.

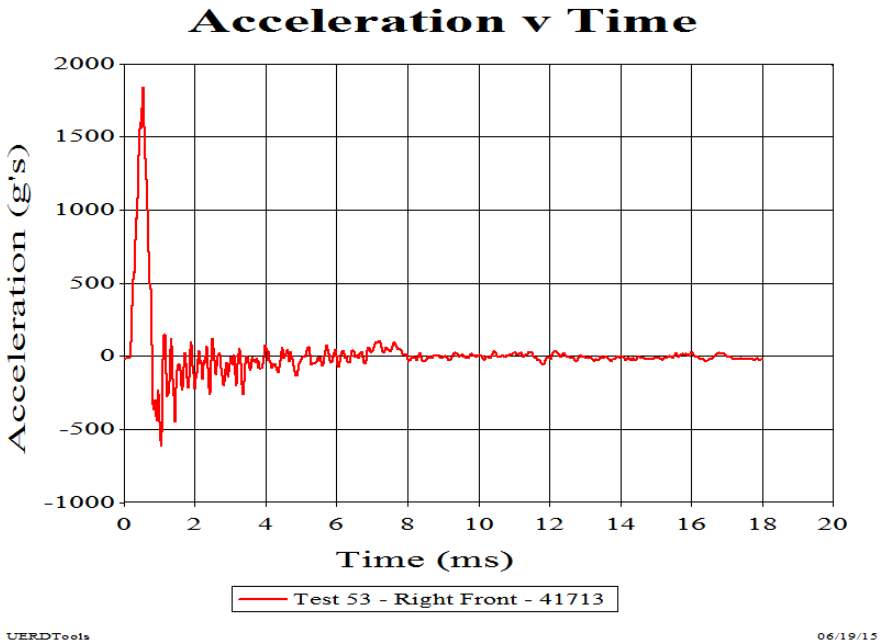

Figure 3.4: Sample acceleration versus time plot

After all four tests were completed, the peak acceleration data was compiled and showed that the combination of the polyurea coated cans and V-bottom hull drastically reduces peak acceleration by 92.1% from the baseline case (flat bottom hull, rigid connection). The scaling factor for these tests is 10, scaling the 4.4 gram charge used in this test to a 10 pound charge at full scale. This scaling factor of 10 also means that a peak acceleration of the small scale plate of 1000 g's corresponds to a full scale acceleration of 100 g's. In this case, the flat hull rigid connection plate experienced an acceleration of 1406 g's, or 140.6 g's on a full scale vehicle. This is certainly dangerous to the soldiers in the vehicle. When both the V-bottom hull and the polyurea coated can connection are employed, the plate is accelerated to only 111 g's, or 11.1 g's at full scale. Table 3.2 presents the data from the centered charge series numerically, while Figure 3.5 presents the data graphically.

Test Number	Charge Location	Hull Shape	Connection	Peak Acceleration (g's)	Reduction from Baseline (%)
1	Center	Flat	Rigid	1406	-
2	Center	Flat	Poly. Coated	936	33.43
3	Center	V-Bottom	Rigid	163	88.40
4	Center	V-Bottom	Poly. Coated	111	92.11

Table 3.2: Test results for flat bottom hull versus V-bottom hull

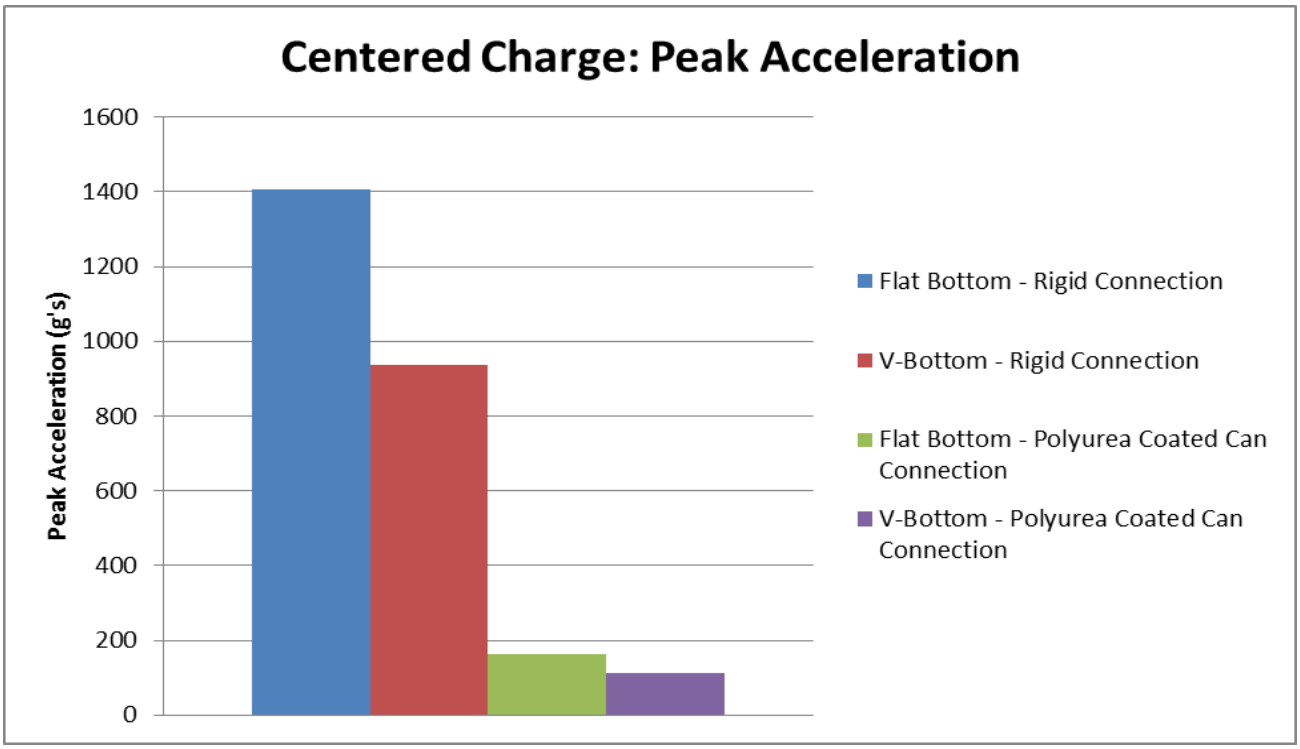

Figure 3.5: Test results for flat bottom hull versus V-bottom hull

The data shows that the polyurea coated cans, even without the V-bottom hull, are a drastic improvement over a rigid connection. An 88% reduction from the baseline case (flat bottom hull, rigid connection) is seen with the flat bottom hull and polyurea coated cans. With a scaling factor of 10, this means that a peak acceleration at full scale of 140 g's is reduced to just 11.1 g's with the use of the V-bottom hull and polyurea-coated can connection.

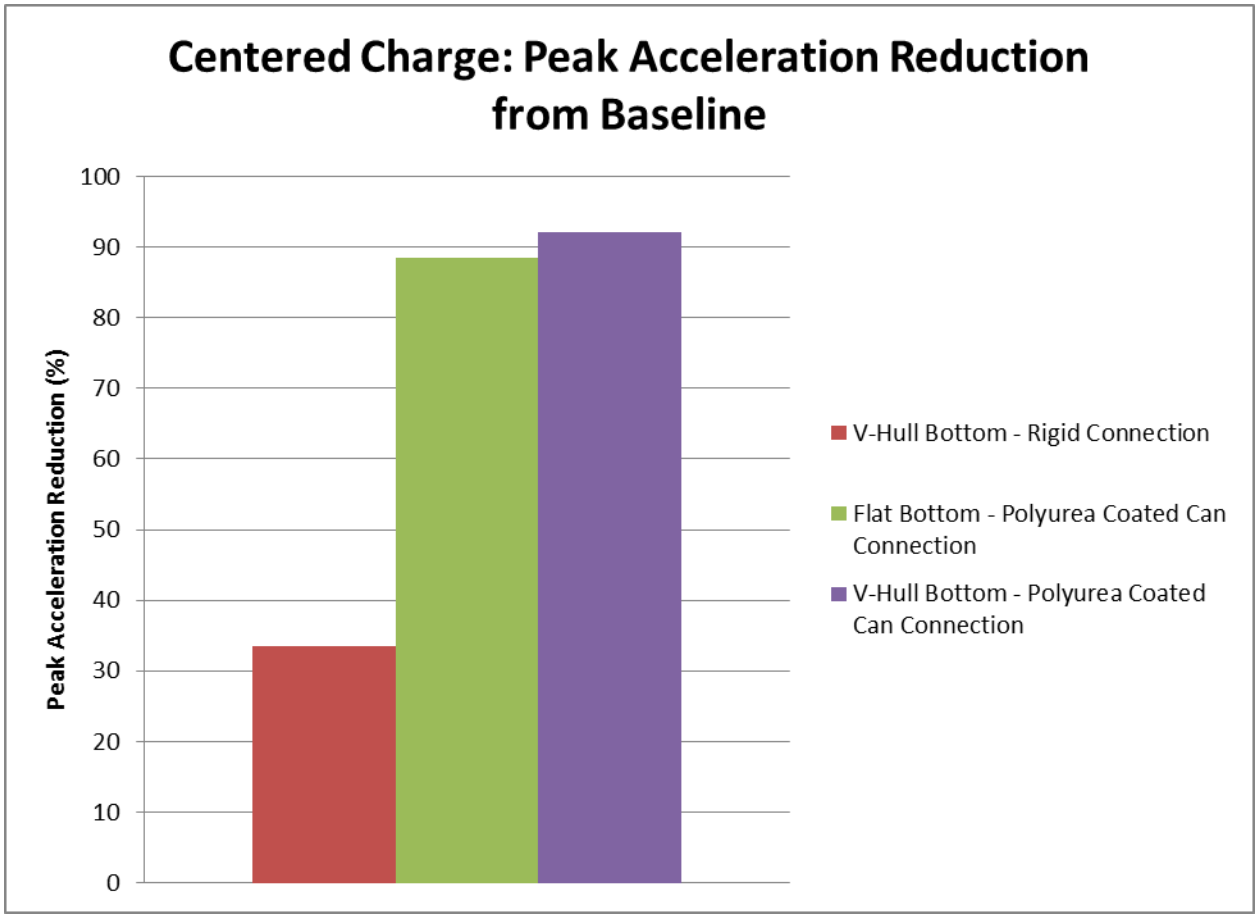

Figure 3.6: Peak acceleration reduction for centered charge location

Figure 3.6 shows the reduction of peak acceleration from the baseline case (flat bottom hull, rigid connection). Clearly, the polyurea-coated can connection has the greatest effect on peak acceleration of a blast loaded vehicle. While the V-bottom

hull by itself reduces peak acceleration by only about 33%, the V-bottom hull in conjunction reduces peak acceleration by greater than 90%. The 33% reduction in peak acceleration by the V-bottom hull alone is in line with previous work done in the Dynamic Effects Lab, where a plate of a matching 20 degree dihedral angle reduced impulse by up to 45% [7].

Chapter 3.1.3 Test Repeatability

A major concern when doing this testing is that the tests are repeatable. Conditions must be identical between tests because you are comparing the tests to each other. To check test repeatability, the V-Bottom, rigid connection test was chosen at random and repeated to see how the data compared. The data can be seen in Table 3.3 below.

Test	Linear Energy (J)	Avg. Velocity (m/s)	Peak Acceleration (g's)
V-Bottom, rigid	24.6	2.02	936
Repeat Test	25.0	2.04	967
Difference (%)	1.6	1.0	3.3

Table 3.3: Test data repeatability for V-bottom, rigid connection

As can be seen in Table 3.3, the tests are very repeatable. The difference is calculated by calculating the difference between the two values, then dividing by the smaller value. Differences of 1.6%, 1.0%, and 3.3% are very small for small scale blast testing. This proves that our test methods and data can be trusted and our tests can be compared with one another in the future.

Chapter 3.2 Effect of Off-Center Charges for Flat and V-Bottom Hull

Once the value of the V-Bottom hull and polyurea coated can was demonstrated for blasts directed at the center of the plate, the techniques were also tested for off-center charges at four locations.

3.2.1 Test Apparatus and Specifics

The four off-center charge burial locations are described as quarter front, half front, quarter right, and half right. Quarter front means that the charge is moved a quarter of the length of the vehicle, from the center line of the vehicle, towards the front. Quarter right means that the charge is moved a quarter of the width of the vehicle, from the center line of the vehicle, towards the right. The charge locations can be seen in Figures 3.7 and 3.8.

Despite the varying charge locations, the charge remains the same as before. A 4.4 gram charge, representing a 10 pound charge at full scale, is buried to a 10 millimeter depth of burial, with a 40 millimeter stand-off distance identical to the tests before. The only variables are the changing of the hull and the connectors. The test matrix can be seen in Table 3.4.

Test Number	Charge Location	Hull Shape	Connector
1	Center	Flat	Rigid
2	Center	V	Rigid
3	Center	Flat	Poly. Coated Cans
4	Center	V	Poly Coated Cans
5	Quarter Front	Flat	Rigid

6	Quarter Front	V	Rigid
7	Quarter Front	Flat	Poly. Coated Cans
8	Quarter Front	V	Poly. Coated Cans
9	Half Front	Flat	Rigid
10	Half Front	V	Rigid
11	Half Front	Flat	Poly. Coated Cans
12	Half Front	V	Poly. Coated Cans
13	Quarter Right	Flat	Rigid
14	Quarter Right	V	Rigid
15	Quarter Right	Flat	Poly. Coated Cans
16	Quarter Right	V	Poly. Coated Cans
17	Half Right	Flat	Rigid
18	Half Right	V	Rigid
19	Half Right	Flat	Poly. Coated Cans
20	Half Right	V	Poly. Coated Cans

Table 3.4: Test matrix for off-center charges study

For these tests, the accelerometer placement was slightly changed from before. One accelerometer was placed directly on the center line of the frame and one accelerometer was placed on the edge of the plate on the "high side", or the side of the plate that the off-center charge is loaded. For example, for the quarter front and half front tests, the "high side" accelerometer was placed at the very front edge of the plate. For the quarter right and half right tests, the "high side" accelerometer was placed at the very right edge of the plate. This was done to measure the acceleration

felt by a soldier in the worst case scenario. The acceleration of the “high side” should be significantly higher than the center of gravity, and seeing the impact that the V-bottom hull and polyurea coated cans can have in mitigating that acceleration is very important. The accelerometer placement, along with charge locations, can be seen in Figures 3.7 and 3.8, as the accelerometer pads are placed on the center line of the frame and “high side” of the frame.

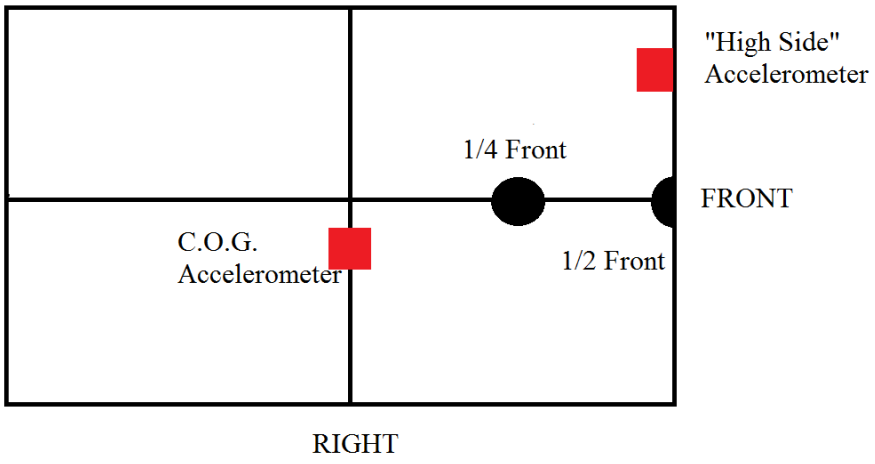

Figure 3.7: Placement of charges and accelerometers for ¼ Front and ½ Front

For the front testing, the accelerometer was not placed directly on the center of gravity but on the center line. The accelerometer does not need to be at the exact center of gravity because the plate should experience the same acceleration at all points along the center line across the width of the plate

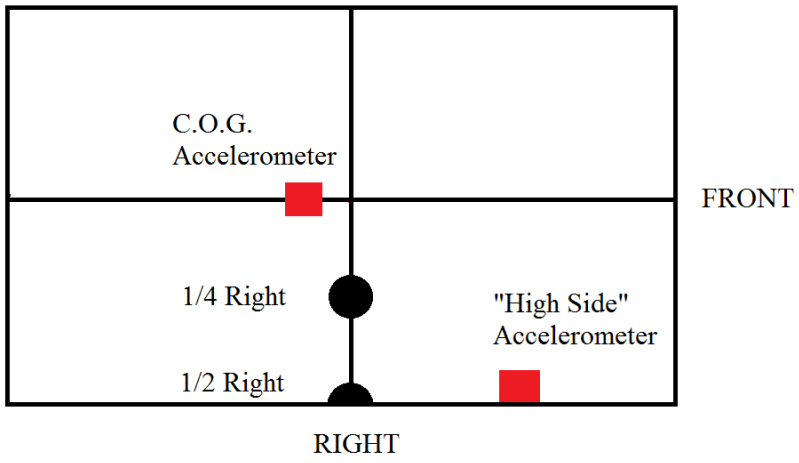

Figure 3.8: Placement of charges and accelerometers for ¼ Right and ½ Right

Figure 3.8 above shows the charge and accelerometer placement for all ¼ Right and ½ Right tests. One accelerometer is placed on the high side, or the side nearest the charge, while the other accelerometer is placed on the center line, similarly to the ¼ Front and ½ Front tests as explained above.

One matter of debate when setting up the off-center charge tests was how to support the plate. Originally, fishing line was used in place of the S-hooks to attach the plate to the chains. Fishing line was used because it would ideally snap as soon as it was loaded and the plate would be able to rotate freely in the air. Upwards of 30 tests were done using multiple different types of fishing line with different break strengths. Unfortunately, despite the large number of tests completed, no consistent data could be gathered. The fishing line would not consistently snap at each support during a test and thus affected the test results. The fishing line would also not consistently snap between tests, meaning that the fishing line would support the plate

longer in some tests relative to others. This provided inconsistent results that could not be used. As before, chains were eventually used to hang the plate. While the chains do not allow for free rotation of the plate, the motion of the plate would be more similar to that of a real vehicle. On a real vehicle, the vehicle's wheels would prevent one end of the vehicle from moving downward, allowing only one end of the vehicle to move upward. A similar effect is seen when the plate is hung from chains, as the "high side" is allowed to travel upwards while the "low side" is constrained from moving downwards by the chains.

3.2.2 Effect of Off-Center Charges for Flat and V-Bottom Hull

A mitigating effect similar to that seen for centered charges is displayed for off-center charges. For the four different charge locations, when utilizing both the V-bottom hull and the polyurea coated cans, the center of gravity peak acceleration is always reduced by over 80%, and frequently over 90%. A great reduction is also seen for the "high side" of the vehicle, where the acceleration of the plate is often much higher than the center of gravity. The data is presented in tabular form in Table 3.5. Figure 3.9 graphically displays the peak acceleration of the center of gravity.

Test Number	Charge Location	Hull Shape	Connector	C.O.G. Peak Acceleration (g's)	Reduction from Baseline (%)
1	Center	Flat	Rigid	1406	-
2	Center	Flat	Poly. Coated	936	33.43
3	Center	V-Bottom	Rigid	163	88.40

4	Center	V-Bottom	Poly. Coated	111	92.11
5	¼ Front	Flat	Rigid	1459	-
6	¼ Front	V	Rigid	1007	30.98
7	¼ Front	Flat	Poly. Coated	599	58.94
8	¼ Front	V	Poly. Coated	118	91.91
9	½ Front	Flat	Rigid	892	-
10	½ Front	V	Rigid	424	52.46
11	½ Front	Flat	Poly. Coated	145	83.74
12	½ Front	V	Poly. Coated	160	82.06
13	¼ Right	Flat	Rigid	1978	-
14	¼ Right	V	Rigid	1296	34.48
15	¼ Right	Flat	Poly. Coated	532	73.10
16	¼ Right	V	Poly. Coated	156	92.11
17	½ Right	Flat	Rigid	811	-
18	½ Right	V	Rigid	481	40.69
19	½ Right	Flat	Poly. Coated	191	76.45
20	½ Right	V	Poly. Coated	94	88.41

Table 3.5: Tabular results of off-center testing for C.O.G. peak acceleration

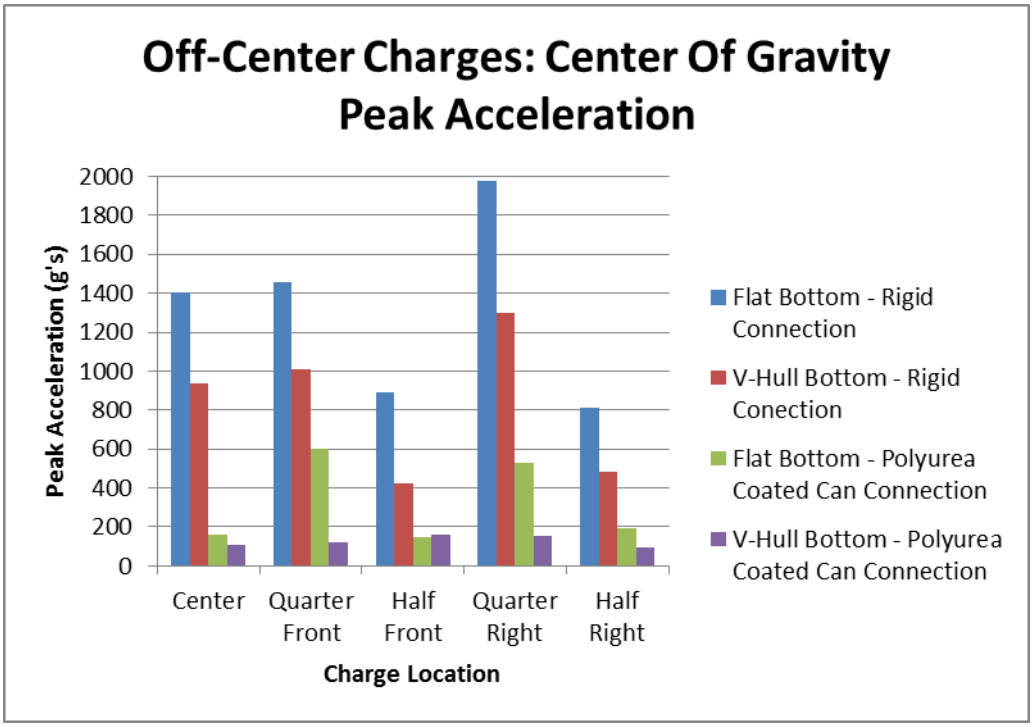

Figure 3.9: Center of gravity peak acceleration data for off center charges

The data shows a trend similar to that seen in the center loading testing. The polyurea-coated can connection, even in conjunction with the flat bottom hull, works better than just the V-bottom hull and the rigid connection. The V-bottom hull with the polyurea coated can connection almost always mitigates more than any other combination, although the discrepancy gets smaller as the charge is moved closer towards the edge of the plate.

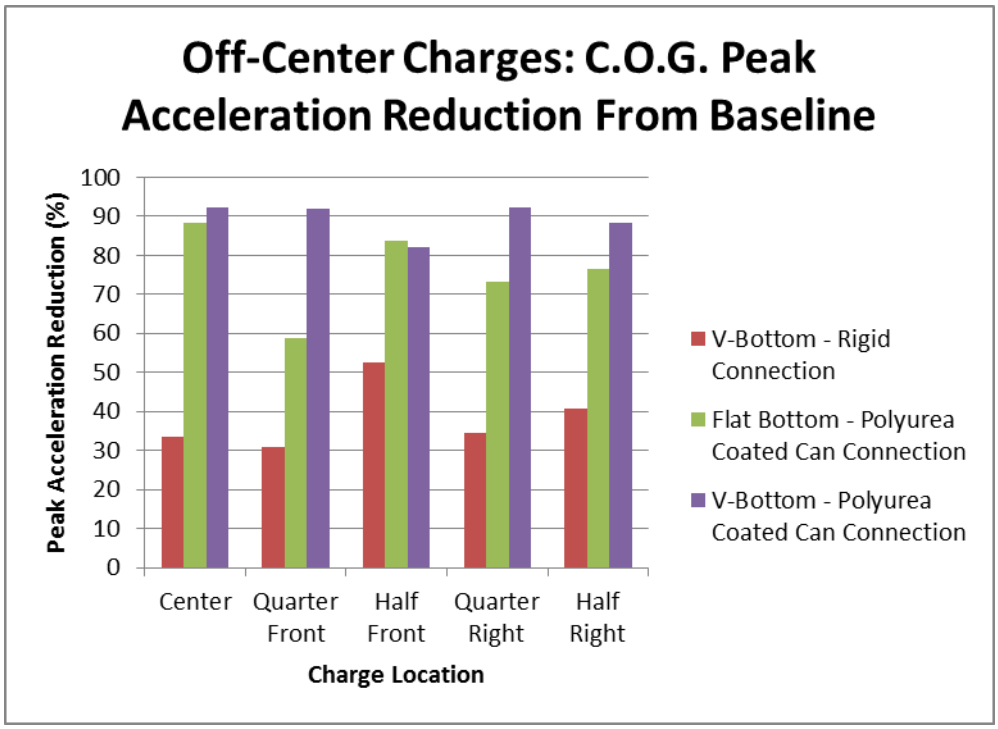

Figure 3.10: Center of gravity peak acceleration reduction from baseline

Figure 3.10 displays the reduction of peak acceleration at the center of gravity for the off-center charges. The harshest baseline center of gravity peak acceleration is seen at the quarter right charge location. At the quarter right charge location, the polyurea-coated cans in conjunction with the V-hull mitigates 93% of acceleration. A peak acceleration of 197.8 g's at full scale is reduced to 15.6 g's, again taking a very violent event and making it survivable.

A similar trend can be seen in the "high side" peak acceleration data. The V-bottom hull in conjunction with the polyurea coated cans is capable of mitigating up to 95% of the peak acceleration. The data can be seen below, tabulated in Table 3.6. Figure 3.11 shows the data in graphical form.

Test Number	Charge Location	Hull Shape	Connector	"High Side" Peak Acceleration (g's)	Reduction from Baseline (%)
5	¼ Front	Flat	Rigid	3600	-
6	¼ Front	V	Rigid	2459	31.0
7	¼ Front	Flat	Poly. Coated	1263	58.9
8	¼ Front	V	Poly. Coated	173	95.2
9	½ Front	Flat	Rigid	2082	-
10	½ Front	V	Rigid	916	56.0
11	½ Front	Flat	Poly. Coated	397	80.9
12	½ Front	V	Poly. Coated	470	77.4
13	¼ Right	Flat	Rigid	3006	-
14	¼ Right	V	Rigid	992	61.8
15	¼ Right	Flat	Poly. Coated	1104	78.7
16	¼ Right	V	Poly. Coated	205	87.7
17	½ Right	Flat	Rigid	1841	-
18	½ Right	V	Rigid	704	40.69
19	½ Right	Flat	Poly. Coated	392	76.45
20	½ Right	V	Poly. Coated	227	88.41

Table 3.6: Tabular results of off-center testing for "high side" peak acceleration

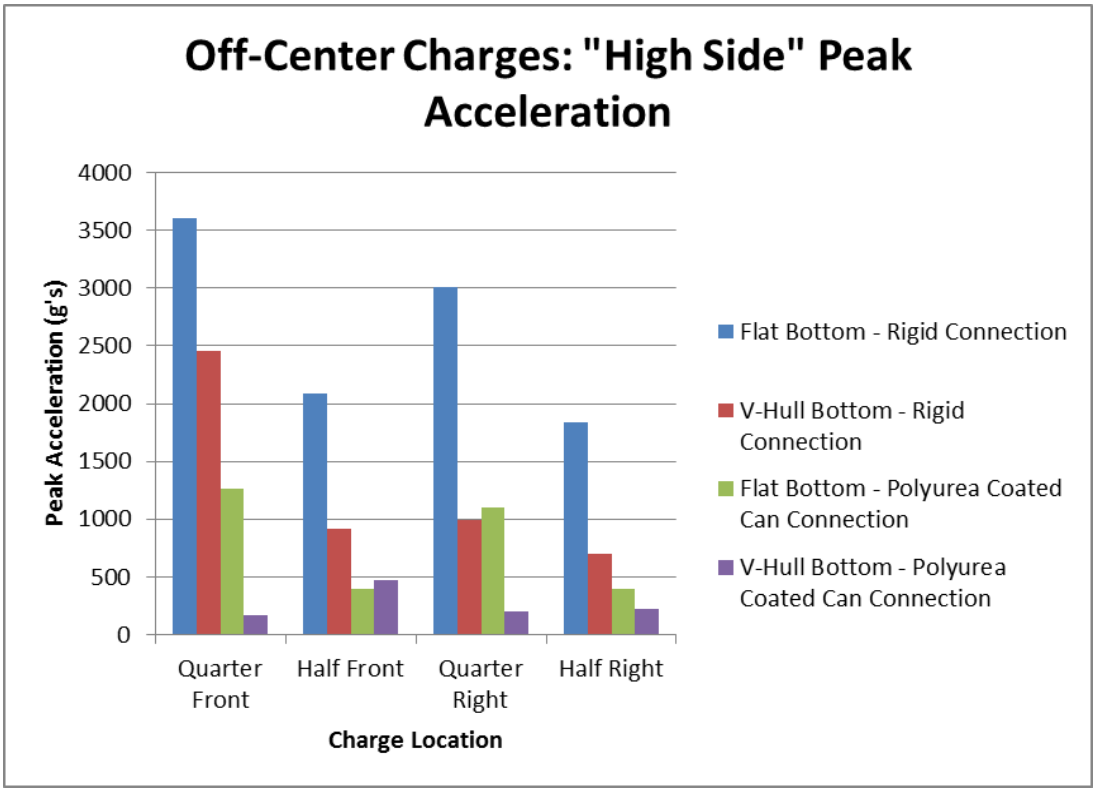

Figure 3.11: Peak acceleration data for the "high side"

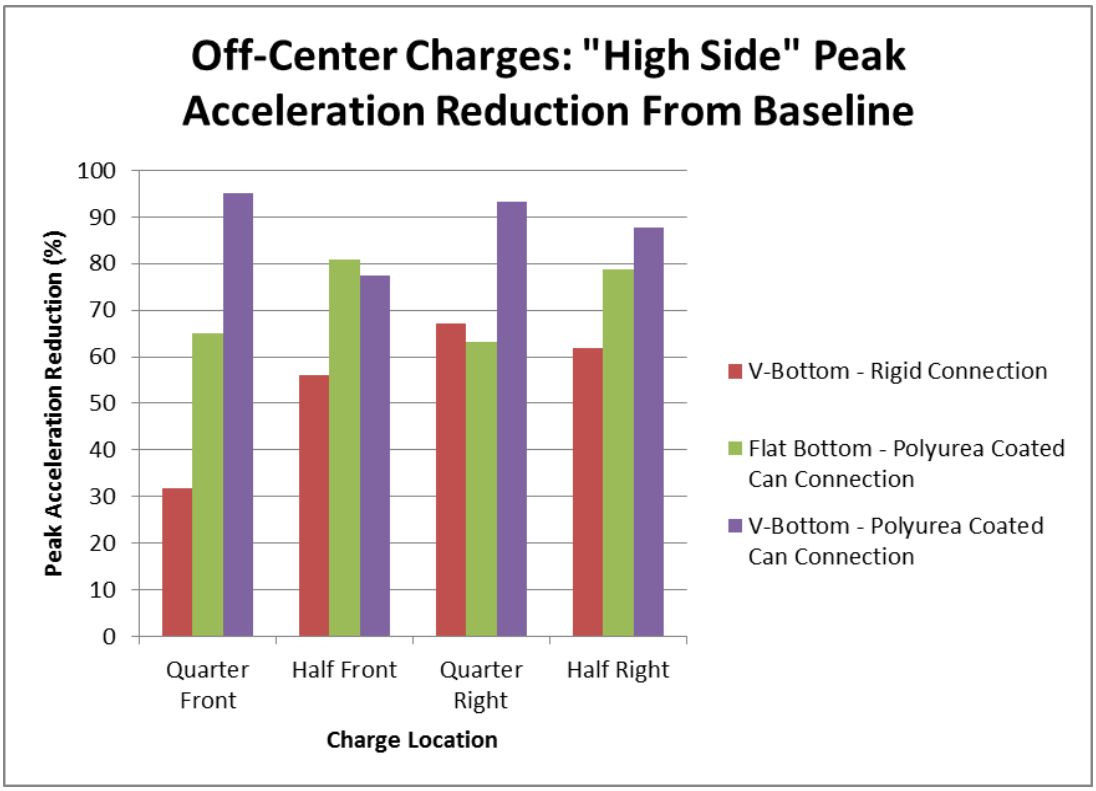

Figure 3.12: Peak acceleration reduction from baseline for the "high side"

Figure 3.12 shows the reduction in peak acceleration from the baseline case for the “high side” In the case of the most extreme “high side” loading condition, at the quarter front charge location, a 3,600 g peak acceleration (360 g’s at full scale) is reduced down to 173 g’s (17.3 g’s at full scale). This 95 percent reduction in peak acceleration is an incredible result. An event that would be extremely traumatic, if not lethal, is reduced to a survivable outcome.

The data displays a clear result: implementing either the V-bottom hull or the polyurea coated cans to mitigate the acceleration on a blast loaded vehicle will be very effective. Using the two mitigation techniques together will typically provide a reduction upwards of 80% from the baseline case (flat bottom hull, rigid connection), in some cases up into the mid 90% range.

Chapter 4 – Conclusion and Future Work

4.1 Conclusion

The purpose of this research was to determine the effect that hull shaping and crushing polyurea-coated thin-walled cylinders could have on mitigating the acceleration felt by personnel in a blast loaded vehicle. Tests were conducted with shaped hulls and crushing polyurea-coated cans, both independently and together, to determine the effects and to see how the two methods worked together compared to apart. Tests were done in saturated sand and with five different charge locations, both centered and off-centered.

The results of the testing were clear: combing the V-bottom hull and polyurea-coated cans was a success. The peak acceleration of the simulated vehicle was almost always reduced by 80-90%, making a dangerous explosive event survivable. In the most extreme case, at full scale, the peak acceleration of a soldier on the simulated vehicle was reduced from 360 g's to 17.6 g's, a 95% reduction. This takes an event that would be very dangerous to an event that is certainly survivable. Implementing these mitigation techniques would not only save lives, but improve the quality of life of soldiers long after they have returned home.

4.2 Suggested Future Work

While this research certainly shed some light on ways to mitigate the acceleration experienced by a blast loaded vehicle, more questions have arisen. One avenue of future work is the continuing research into nested cans and their

effectiveness. Nested cans of a shorter height were constructed and were tested as a supplementary goal for this testing, but no conclusive data could be gathered and the data could not be included in this research. These tests were conducted both with and without polyurea coating. Nested cans and their effectiveness are certainly a promising technology, but more time and testing is required to understand their behavior.

Finally, research into other ways to mitigate blast loading on vehicles without increasing vehicle height can be explored. Previous work in the Dynamic Effects Lab briefly explored crushing thin tubes rather than thin-walled cylinders. It is certainly possible that other methods could equally mitigate acceleration on a vehicle without adding so much height to the vehicle.

Bibliography

[1] Nelson, N.W., Lamberty, G.J., Sim, A.H., Doane, B.M. "Blast from the Past and Present: A Review of Blast-Related Injury in Military Personnel and Veterans." *Neuropsychological Practice with Veterans* (2012): 145.

[2] Fiskum, G., Hazelton, J., Gullapalli, R., Fourney, W.L. "Animal Model of Mild Brain Injury Caused by Blast-Induced Hyper-Acceleration Relevant to IED-Targeted Military Vehicles."

[3] Lamb, C., Schmidt, M., Fitzsimmons, B. "MRAPS, Irregular Warfare, and Pentagon Reform." Institute for National Strategic Studies National Defense University. Volume 6, June 2009.

[4] Bagalman, E. (2015, March 9). Health Care for Veterans: Traumatic Brain Injury. Retrieved June 19, 2015, from https://www.fas.org/sgp/crs/misc/R40941.pdf

[5] Bryan, M., & Andrew, S. (2008, July 1). SF deaths come amid MRAP rollover concerns. Army Times. Retrieved June 19, 2015, from http://archive.armytimes.com/article/20080701/NEWS/807010311/SF-deaths-come-amid-MRAP-rollover-concerns

[6] Fourney, W. L., Leiste, U., Bonenberger, R., Goodings, D. J. "Mechanism of Loading on Plates Due to Explosive Detonation." Fragblast, Vol. 9, No. 4, December 2005.

[7] Genson, K. (2006). "Vehicle Shaping for Mine Blast Damage Reduction." University of Maryland: College Park.

[8] Benedetti, R., Fourney, W.L. (2010) "Mitigation of Loading on Floorboards in Light Armored Vehicles Subjected to Explosive Loading." University of Maryland: College Park.

[9] Leiste, U. (2012). "Experimental Studies to Investigate Pressure Loading on Target Plates." University of Maryland: College Park.

[10] Alghamdi, A.A.A. "Collapsible Impact Energy Absorbers: An Overview." Thin Walled Structures, Vol. 39, No. 2, February 2001.

[11] Yuen, S.C., Nurick, G.N. "The Energy-Absorbing Characteristics of Tubular Structures with Geometric and Material Modifications: An Overview." Applied Mechanics, Vol. 69, No. 2, March 2008.

[12] Gupta, N.K., Sekhon, G.S., Gupta, P.K. "Study of lateral compression of round metallic tubes." Thin Walled Structures, Vol. 43, No. 6, December 2005.

[13] Palanivelu, S., Van Paepegem, W., Degrieck, J., Van Ackeren, J., Kakogiannis, D., Van Hemelrijck, D., Wastiels, J., Vantomme, J. "Experimental study on the axial

crushing behavior of pultruded composite tubes." Polymer Testing, Vol. 29, No. 2, April 2010.

[14] Palanivelu, S., Paepegem, W.V., Degrieck, J., Vantomme, J., Kakogiannis, D., Ackeren, J.V., Hemelrijck, D.V., Wastiels, J. "Comparison of the crushing performance of hollow and foam-filled small-scale composite tubes with different geometrical shapes for use in sacrificial cladding structures." Composites Part B: Engineering, Vol. 41, No. 6, September 2010.

[15] Palanivelu, S., Van Paepegem, W., Degrieck, J., Reymen, B., Ndambi, J.M., Vantomme, J., Kakogiannis, D., Wastiels, J., Hemelrijck, D.V. "Close-range blast loading on empty recyclable metal beverage cans for use in sacrificial cladding structure." Engineering Structures, Vol. 33, No. 6, June 2011.

[16] Theobald, M.D., Nurick, G.N. "Numerical investigation of the response of sandwich-type panels using thin-walled tubes subject to blast loads." International Journal of Impact Engineering. Vol. 34, No.1, January 2007.

[17] Theobald, M.D., Nurick, G.N. "Experimental and numerical analysis of tube-core claddings under blast loads." International Journal of Impact Engineering. Vol. 37, No.3, March 2010.

[18] Roland, C.M., Twigg, J.N., Vu, Y., Mott, P.H. "High Strain Rate Mechanical Behavior of Polyurea." Polymer, Vol. 48, No.2, January 2007.

[19] Tekalur, S.A., Shukla, A, Shivakumar, K. "Blast resistance of polyurea based layered composite materials." Composite Structures, Vol. 84, No.3, July 2008.

[20] Yi, J., Boyce, M.C., Lee, G.F., Balizer, E. "Large deformation rate-dependent stress-strain behavior of polyurea and polyurethanes." Polymer, Vol. 47, No.1, January 2006.

[21] Brodrick, T.J. "Mitigation of Frame Acceleration Induced by a Buried Charge." Diss. 2010.

[22] Bonsmann, J. (2013) "Small-scale testing to study mitigation of acceleration on simulated vehicles." University of Maryland: College Park.

[23] Fourney, W. L., Leiste, U., Bonenberger, R., Goodings, D. J. "Explosive Impulse on Plates." Fragblast, Vol. 9, No. 1, December 2005.

[24] Taylor, L.C., Skaggs, R.R., Gault, W. "Vertical Impulse Measurement of Mines Buried in Saturated Sand." Fragblast, Vol. 9, No.1, March 2005.

[25] PCB Piezotronics, Shock ICP Model: 350B04. (2013). Retrieved August 20, 2013 from http://www.pcb.com/products.aspx?m=350B04#.UhOiuZLVAsI

[26] Bonsmann JM, Fourney WL (2012) An examination of the factors affecting the loading on a vehicle subjected to the detonation of a buried mine. Blast Fragm 6(3):155–180

[27] RP-501 Economy EBW Detonator. (2011). Retrieved August 20, 2013 from http://www.teledynerisi.com/products/0products_1ebw_page28.asp